Reviewed research article

The 1845–46 and 1766–68 eruptions at Hekla volcano: new lava volume estimates, historical accounts and emplacement dynamics

Rikke Vestergaard[1*], Gro Birkefeldt Møller Pedersen[2,3] and Christian Tegner[1]

[1]*Aarhus University, The department of Geoscience, Centre of Earth System Petrology*

[2]*Institute of Earth Sciences, University of Iceland, Reykjavík, Iceland*

[3]*Nordic Volcanological Center, University of Iceland, Reykjavík, Iceland*

[*]*Corresponding author: rikke.vest94@gmail.com*

https://doi.org/10.33799/jokull2020.70.035

Abstract — *We use new remote sensing data, historical reports, petrology and estimates of viscosity based on geochemical data to illuminate the lava emplacement flow-lines and vent structure changes of the summit ridge of Hekla during the large eruptions of 1845–46 and 1766–68. Based on the planimetric method we estimate the bulk volumes of these eruptions close to 0.4 km^3 and 0.7 km^3, respectively. However, comparison with volume estimates from the well-recorded 1947–48 eruption, indicates that the planimetric method appears to underestimate the lava bulk volumes by 40–60%. Hence, the true bulk volumes are more likely 0.5–0.6 km^3 and 1.0–1.2 km^3, respectively. Estimated melt viscosity averages for the 1766–68 eruption amount to 2.5 $\times$ 10^2 Pa s (pre-eruptive) and 2.5$\times$10^3 Pa s (degassed), and for the 1845–46 eruption 2.2$\times$10^2 Pa s (pre-eruptive) and 1.9$\times$10^3 Pa s (degassed). Pre-eruptive magmas are about one order of magnitude more fluid than degassed magmas. In the 1845–46 and 1947–48 eruptions, SiO_2 decreased from 58–57 to 55–54 wt% agreeing with a conventional model that Hekla erupts from a large, layered magma chamber with the most evolved (silica-rich) magmas at the top. In contrast, the lava-flows from 1766–68 reveal a more complicated SiO_2 trend. The lava fields emplaced in 1766 to the south have SiO_2 values 54.9–56.5%, while the Hringlandahraun lava-flow that erupted from younger vents on the NE end of the Hekla ridge in March 1767 has higher SiO_2 of 57.8%. This shows that the layered magma chamber model is not suitable for all lava-flows emplaced during Hekla eruptions.*

INTRODUCTION

The Hekla volcano is one of the four most active volcanic systems in Iceland, having erupted about 23 times since the settlement of Iceland in the year 874 (Thórarinsson, 1967; Thordarson and Larsen, 2007; Höskuldsson *et al.*, 2007; Pedersen *et al.*, 2018a,b). Hekla therefore presents one of the major volcanic hazards of Iceland (Einarsson, 2018; Barsotti *et al.*, 2019). So far, the older historical eruptions have mainly been studied from literary sources in combination with tephra chronology, which provides a great record of the explosive activity and its related hazards (Thórarinsson, 1967; Sverrisdottir, 2007; Gudnason *et al.*, 2017, 2018; Janebo *et al.*, 2016a,b, 2018). Hekla eruptions generally start with subplinian to plinian explosive eruption plumes up to 12–36 km high (Thorarinsson, 1967; Höskuldsson *et al.*, 2007), and typically gives no to little warning (Grönvold *et al.*, 1983; Soosalu *et al.*, 2003; Einarsson, 2018). This makes future Hekla eruptions hazardous for air traffic, especially since one of the busiest air traffic corridors in the world runs straight over Hekla (Soosalu *et al.*,

2003; Gudnason *et al.*, 2017; Janebo *et al.*, 2018, Einarsson, 2018; Barsotti *et al.*, 2019). The effusive eruption of Hekla lavas also represent a hazard for the surrounding settlements and farmland, but has remained understudied in particular the lavas erupted before the 20th century (Jakobsson, 1979; Pedersen *et al.*, 2018b). There is therefore sparse information regarding lava-flow emplacement, lava morphology and lava volumes. For example, the eruptions in 1845–46 and 1766–68 are some of the largest known eruptions from Hekla since the settlement. They are comparable in volumes to the 0.4 km^3 eruption of Surtsey 1963–67 (lava shield part) and to the recent 1.44 km^3 2014–15 eruption of Holuhraun, respectively (Thórarinsson, 1967; Thordarson, 2000; Thordarson and Larsen, 2007; Janebo *et al.*, 2016a,b; Pedersen *et al.*, 2017, 2018a,b; Bonny *et al.*, 2018; Gudnason *et al.*, 2018). Previous work has concluded that Hekla's plumbing system involves a single, zoned magma source and that the most silica-rich magmas (rhyolite) are tapped from the topmost layer during the initial explosive phase (particularly the case for prehistoric eruptions) (Sigmarsson *et al.*, 1992; Sverrisdottir, 2007). During the subsequent effusive eruptions the SiO_2 of the erupted melts declines towards basaltic andesite (ca. 54 wt%) (Sigmarsson *et al.*, 1992; Thordarson and Larsen, 2007). Following this hypothesis, a negative correlation of silica content and relative emplacement age is expected during eruptions. The aim of the present study is to extend the understanding of the effusive activity at Hekla using remote sensing data, petrology, geochemistry (with focus on whole rock SiO_2 values and their correlation with relative lava emplacement age, and on estimating viscosity) and historical sources of the 1845–46 and 1766–68 eruptions. The two eruptions are selected to improve knowledge of large, effusive activity of Hekla. The 1947–48 eruption is also included as a benchmark since its activity and eruptive products have already been extensively recorded (e.g. Thórarinsson, 1976, Pedersen *et al.*, 2018a). In particular, the goals are to (i) estimate the erupted volumes; (ii) qualitatively outline the emplacement time-lines of the lava-flows; (iii) discuss lava morphology and viscosity, and (iv) discuss magma chamber dynamics of these eruptions.

BACKGROUND

The volcano Hekla

The volcano Hekla is located in the southern part of Iceland at the intersection of the South Iceland Seismic Zone (SISZ) and the Eastern Volcanic Zone (EVZ) (Sæmundsson, 1978; Jakobsson, 1979) (Figure 1). The Hekla volcanic system consists of a NE-SW trending fissure swarm and a central volcano ranging from basalt to rhyolite in composition (Thórarinsson, 1967; Jakobsson, 1979; Sigmarsson *et al.*, 1992; Sverrisdottir, 2007; Larsen *et al.* 2013; Tuller-Ross *et al.*, 2019). Today the central volcano forms a 5–6 km elongated steep-sided ridge that reaches a height of 1490 m a.s.l., superimposed on a basaltic base and oriented parallel to the 60 km NE-SW fissure swarm (Sæmundsson, 1978; Jakobsson, 1979). The nature of the magma chamber beneath the central volcano has been debated. Most authors argue that the changing compositions of the tephras from rhyolite to basaltic andesite demonstrate tapping of a chemically-stratified magma chamber (Sigmarsson *et al.*, 1992; Sverrisdottir, 2007). Sigmarsson *et al.* (1992) initially argued for a very large (20 km long, 5 km wide and ca. 7 km deep) magma chamber with the top ca. 8 km below the surface. Subsequently others have suggested slightly modified architectures such as a dyke-formed magma chamber (Sverrisdottir, 2007) or separate small, connected magma chambers undergoing closed and/or open system geochemical evolution (Chekol *et al.*, 2011). Recent geophysical models confirm that the magma chamber is indeed very deep, probably at depths exceeding 10 km (Ofeigsson *et al.*, 2011; Geirsson *et al.*, 2012; Sturkell *et al.*, 2013). Whereas the tephras range from rhyolite (ca. 75 wt% SiO_2) to andesite (ca. 57 wt% SiO_2) (Sigmarsson *et al.*, 1992; Sverrisdottir, 2007; Janebo *et al.*, 2018), the compositional range of the lavas is more restricted from andesite (ca. 58 wt% SiO_2) to basaltic andesite (ca. 54 wt% SiO_2), which is the typical end composition (Thórarinsson, 1967; Sigmarsson *et al.*, 1992; Larsen *et al.*, 1999; Sverrisdottir, 2007). All the major eruptions occur in the main fissure along the summit ridge, and historical sources describe how the ridge sometimes split in two during eruptions; more complex fissure opening have also been described (Thór-

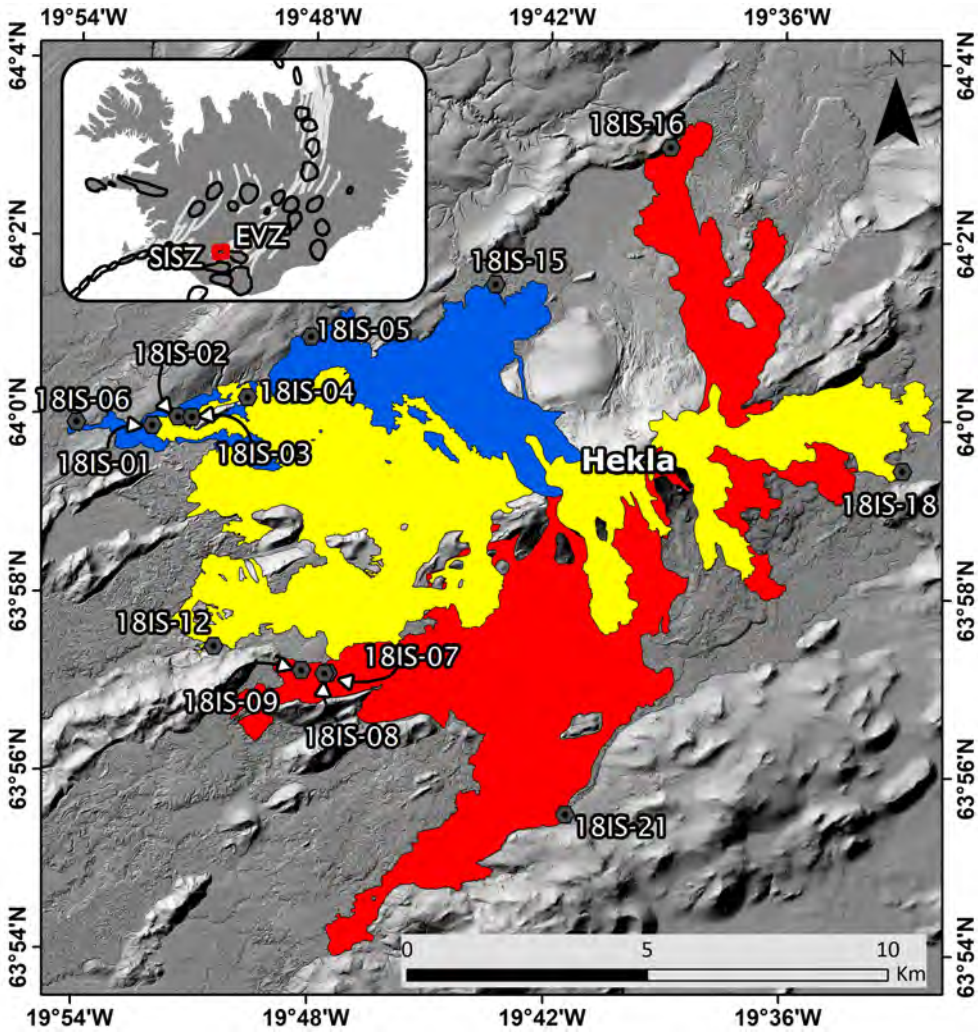

Figure 1. Map of the Hekla lava-flow fields 1947–48 (yellow), 1845–46 (blue) and 1766–68 (red). Locations of field samples are shown as black/gray hexagon dots and noted with sample names. Background shows hillshade from smoothed lidar DEM with gaps filled with TDX DEM (Rizzoli *et al.*, 2017; Pedersen *et al.*, in prep.). The boundary outlines of the lava-flow fields are provided by Pedersen *et al.* (2018b). The inset of Iceland shows volcanic systems (fissure swarms in light gray and central volcanoes in black outlines) according to Einarsson and Sæmundsson (1987). SISZ and EVZ stand for the South Iceland Seismic Zone and Eastern Volcanic Zone. The red frame denotes the Hekla area. – *Kort af Hekluhraunum frá 1947–48 (gul), 1845–46 (blá) og 1766–68 (rauð). Sýnatökustaðir eru sýndir sem svartir/gráir sexhyrndir, númeraðir punktar. Hæðarlíkanið í bakgrunni kortsins er samsett af lidar gögnum og TDX hæðarlíkaninu þar sem göt eru í lidar gögnunum (Pedersen o.fl., í vinnslu; Rizzoli o.fl., 2016). Útlínur hraunbreiðanna eru frá Pedersen o.fl. (2018b). Íslandskortið sýnir sprungusveima (gráir flákar) og megineldstöðvar (svartir hringir), samkvæmt gögnum frá Páli Einarssyni og Kristjáni Sæmundssyni (1987). SISZ táknar Suðurlandsskjálftabeltið og EVZ er Austurgosbeltið. Rauði ramminn sýnir staðsetningu stóra kortsins.*

arinsson, 1967; Larsen *et al.*, 2013; Pedersen *et al.*, 2018b). In Holocene times, Hekla has mainly produced mixed eruptions which encompasses both explosive and effusive activity (Thordarson and Larsen, 2007; Thordarson and Höskuldsson, 2008; Pedersen *et al.*, 2018b). The eruptions in 1947–48, 1845–46 and 1766–68 were no exceptions (Figure 1). All three behaved rather similarly, exhibiting a highly explosive subplinian to plinian initial phase (VEI 4) with significant tephra fallout (Houghton *et al.*, 2013; Janebo *et al.*, 2016a; Gudnason *et al.*, 2018). The following phases were: fire fountaining, strombolian activity ending with an effusive phase generating large lava-flow fields (Thórarinsson, 1967, 1976; Larsen *et al.*, 1999; Thordarson and Larsen, 2007; Thordarson and Höskuldsson, 2008; Pedersen *et al.*, 2018b). The 1947–48 and 1766–68 eruptions also showed examples of renewed, violent explosivity during the effusive phase, but these events never increased to the same force as the initial phase (Thórarinsson, 1967, 1976).

Lava-flow morphology

Lava is a common and persistent threat to settlements and understanding its properties and emplacement mechanisms is key for hazard assessment and for predicting lava-flow behaviour and development (Soule *et al.*, 2004; Takagi and Huppert, 2010; Montalvo, 2013). This includes the estimation of lava-flow thickness, volume and emplacement style and history (e.g. Wadge *et al.*, 1975; Stevens *et al.*, 1999; Harris *et al.*, 2000; Poland, 2014; Albino *et al.*, 2015; Kubanek *et al.*, 2017; Pedersen *et al.*, 2018a). The development and emplacement of lava-flows hinge on parameters such as rheology, effusion rate and eruption duration, temperature, topography and surface slopes and also total volume of lava extruded (Walker, 1973; Pinkerton and Wilson, 1994; Parfitt and Wilson, 2008). Furthermore, the rheology of the lava evolves during emplacement, because of changes in melt composition, oxygen fugacity and temperature of the magma resulting from gas loss, cooling and crystallisation (Hulme, 1974; Fink, 1980; Gregg and Fink, 2000; Kilburn, 2004; Kolzenburg *et al.*, 2018). Hekla typically generates ʻaʻā lavas (Thórarinsson and Sigvaldason, 1972; Grönvold *et al.*, 1983; Höskuldsson *et al.*, 2007; Thordarson and Höskuldsson, 2008) which are flows with autobrecciated exteriors and a coherent liquid interior during emplacement, referred to as the core. The autobreccia comprises irregular clinkers that have rough, sharp surfaces, and are derived from the flow core (Macdonald, 1953). Common morphologies that are mentioned in this study, are sheet-flows which formed in a single surge of lava that is not bounded by levées (banks of solidified lava), and channelised flows of lava bounded between levées (Hulme, 1974; Peterson and Tilling, 1980; Rowland and Walker, 1988; Hon *et al.*, 1994; Harris *et al.*, 2009; Harris and Rowland, 2015). Morphologies related to lava inflation include flat-surfaced plateaus (formed like tumuli) called lava rise, collapsed depressions called lava-rise pits, and marginal fractures called lava-inflation clefts (Walker, 1991). They form by the injection of lava beneath the surface layer which leads to simple uplift of the surface without any horizontal compression (Walker, 1991). The lava-rise pits and lava-inflation clefts describe, respectively, lava surfaces that failed to be uplifted, and actively inflating interior of the lava-flow that detaches from the stagnated margin (Walker, 1991; Hon *et al.*, 1994). Inflation structures are commonly found in pāhoehoe flows (e.g. Macdonald, 1953; Walker, 1991, Hon *et al.*, 1994), but inflation structures and lava tubes also occur in ʻaʻā flows (e.g. Calvari and Pinkerton, 1998, 1999; Pedersen *et al.*, 2017). Lava tubes are insulated conduits of still-molten lava beneath a cooler (ultimately solidified) surface layer (Peterson *et al.*, 1994). The boundary of the inflated lava-flow may breach, thus allowing lava breakouts and thereby new lava lobes. Breakouts do not only occur due to rupture of the cooled skin at weak points, but can also occur due to effusion rate fluctuations (Thordarson and Self, 1998; Rowland and Harris, 2015; Pedersen *et al.*, 2017). The emplacement of breakouts may vary depending on viscosity and effusion rate.

DATA AND METHODS

Remote sensing data and bulk volume estimates

The remote sensing data consists of orthophotos and digital elevation models (DEMs) from 1945–46, 1960 and 2015 (Table 1). The remotely-sensed images

Table 1. Overview of remote sensing data sources used for this study of the Hekla lavas 1766–68, 1845–46 and 1947–48. – *Yfirlit yfir fjarkönnunargögn sem notuð voru til að rannsaka Hekluhraunin frá 1766–68, 1845–46 og 1947–48.*

Acquisition	Source	Data (Resolution and m/pixel)	Reference
23 Sep. 1945 & 20 Sep. 1946	Aerial photographs	Ortho (1) + DEM (10)	Pedersen *et al.*, 2018a
20 July 1960 & 4 Aug. 1960	Aerial photographs	Ortho (0.5) + DEM (5)	Pedersen *et al.*, 2018a
Mosaic 2011–2013	TanDEM	DEM (12)	Rizzoli *et al.*, 2017
29 Aug. – 4 Sep. 2015	Aerial photographs & lidar	Ortho (0.2) + DEM (1)	Pedersen *et al.* (in prep.)

and data are processed in the geographic information system program, ArcGIS. The orthophotos and DEMs were provided by Pedersen *et al.* (2018a), and were created using digital photogrammetric techniques generated from repeated aerial stereophotogrammetric surveys conducted over Hekla since 1945 (see Pedersen *et al.*, 2018a). The orthophotos from 1945–46 are particularly important because they reveal the full extent of the 1845–46 lava-flow field and large parts of the 1766–68 lava-flow field before being partly covered by the lavas from the 1947–48 eruption and later eruptions. The DEM from 2015 is mainly applied for the planimetric method (see below), except for areas covered by younger flows, e.g. the southern lava-flows of the 1766–68 eruption. Where younger lava-flows cover the 1766–68 and 1845–46 lava-flow fields, the 1945-46 DEM is used, and where the 1947–48 lava-flow field is covered by younger lava-flows, the 1960 DEM is applied. Moreover, maps delineating Hekla's lava units (inclusive the 1766–68 and 1845–46) are provided by Pedersen *et al.* (2018b) (Figure 1).

The planimetric method (Stevens *et al.*, 1999) is the only available approach to estimate the bulk volumes of the 1766–68 and 1845–46 eruptions. We follow the example of Montalvo (2013) who also used the planimetric approach to estimate volumes for the Hekla lava-flow fields from the eruptions in 1878, 1913 and 1980–81. Similarly, the recent investigation of El Reventador Volcano, Ecuador by Naranjo *et al.* (2016) also used the planimetric method together with topographic satellite radar-based measurements to better distinguish between different lava-flow eruptions from the total lava volume change from 2002–2009. The bulk volume is calculated by multiplying the area covered by lava with an estimated mean lava thickness. The planimetric method works best if the flow field is divided into morphological zones where the thickness can be assumed relatively constant (Montalvo, 2013). These morphological zones are mapped based on orthophotos and slope maps from post-eruption DEMs. The area is extracted for each zone (Figure 2f). Thickness estimates are obtained by calculating the average thickness based on multiple thickness measurements of profiles along the lava-flow margins (Figure 2a). To obtain reliable thickness estimates, it is important that the area outside the flow field is fairly flat, and we decide that thickness is extracted from the profiles as soon as the lava-flow flattens, thus remaining consistency throughout our thickness measurement extractions (Figure 2b,c,d,e). For zones where no thickness estimates could be obtained, e.g. zones on steep slopes, the average of all the other zone thicknesses are used instead.

Historical sources and emplacement time-lines

The historical sources include primarily the study by the Icelandic volcanologist Sigurdur Thórarinsson (1912–1983) who carried out extensive work on Hekla (Thórarinsson, 1967, 1976; Björnsson, 1983), and secondarily descriptions by Danish geologist Jørgen Christian Schythe (1814–1877) and Hans Finnsen (1739–1796) (Finnsen, 1767; Schythe, 1847; Thórarinsson, 1967; Bricka, 2019). Sigurdur Thórarinsson collected and summarised literary sources and compiled them into a chronological account of Hekla eruptions from 1158 to 1947. The narratives from J.C. Schythe and H. Finnsen recount the 1845–46 and 1766–68 eruptions, respectively. It should be noted that H. Finnsen did not witness the beginning of the 1766–68 eruption (April 5, 1766) as he was in Copenhagen, but he arrived on July 16, 1766 at Skálholt

some 40 km NW of Hekla, where his father was bishop, and from then on followed the eruption. Thus, the accounts of the initial phases of the eruption was based on Einar Jónsson (1712–1788) (Thórarinsson, 1967). Thórarinsson (1967) is used in this study as a "historical source" as it includes several accounts and interpretations of previous eyewitness-narratives of the eruptions, e.g. Einar Jónsson (1712–1788) (mentioned above) and Rev. Sveinn Vigfússon (1732–1766). Since we have had access to the Danish-

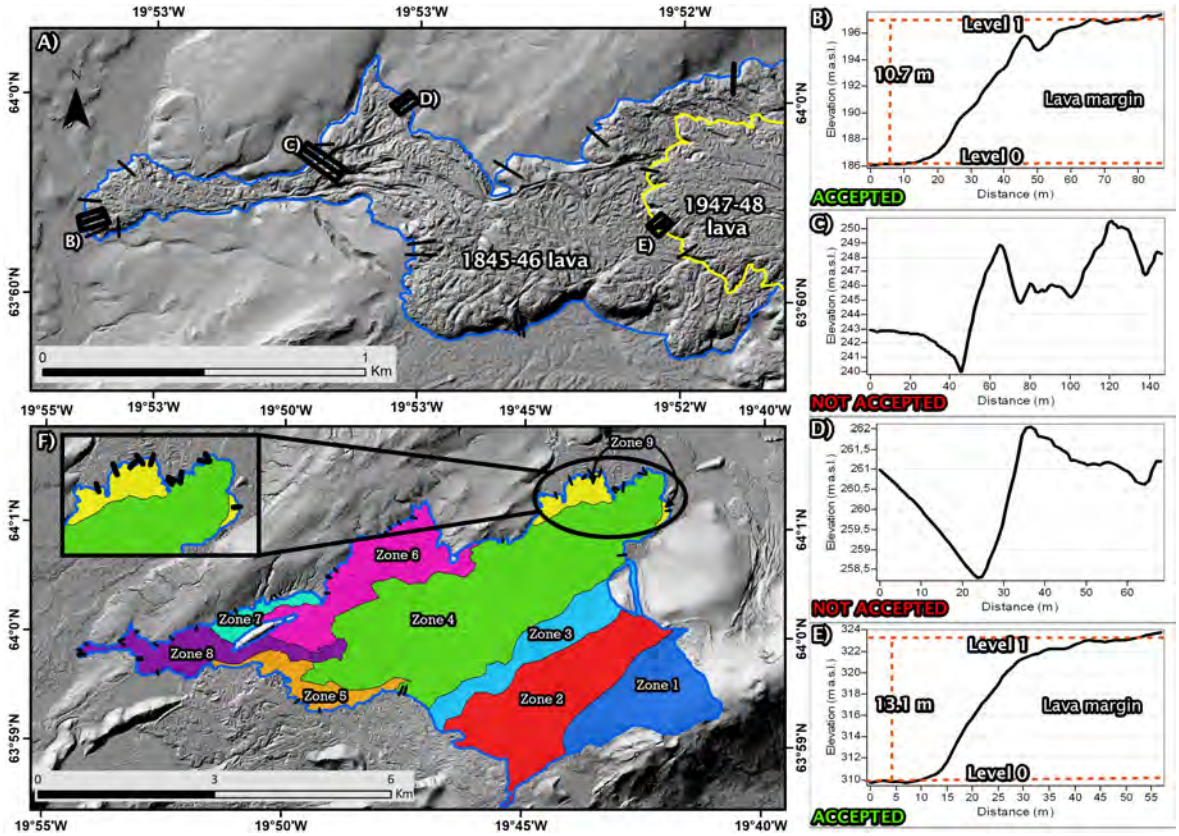

Figure 2. A) An illustration of lava thickness measurements comprising examples of elevation profiles B), C), D) and E) that meets and does not meet the requirements for lava thickness measurements. These are respectively marked by accepted or not-accepted in the bottom left of the profile. The base of the flow marks level 0. It is assumed that the thickness of the lava is reached at the level where the steep slope of the lava front levels off. This marks level 1. The difference in elevation between level 1 and level 0 is taken as the thickness of the flow for that particular profile. Average thicknesses are estimated from the accepted profile graphs and are used in the bulk volume calculations. F) Map of the 1845–46 lava-flow field delineated into nine zones, and close-up of thickness profile measurements marked with black lines. Zone 1: vent area, complex morphology changing into channelised flows (approx. slope of area: $\leq 55°$). Zone 2: complex morphology changing into channelised flows ($\leq 40°$). Zone 3: lava-falls with complex narrow channels ($\leq 40°$). Zone 4: channelised flows ($\leq 15°$). Zone 5 and 6: large inflation structure and breakouts though mostly clear in zone 5 ($\leq 15°$). Zone 7 and 9: breakout ($\leq 10°$). Zone 8: channelised flows and possibly inflation and breakout ($\leq 10°$). Background and boundary outlines as in Figure 1.

written descriptions by J. C. Schythe and H. Finnsen, we interpret them ourselves instead of relying solely on Thórarinsson (1967). Because the present study focuses on the effusive activity, descriptions of lava-flows in the literary sources (Finnsen, 1767; Schythe, 1847; Thórarinsson, 1967) are mainly taken into account. This entails specific time/periods and locations of the effusive activity. Furthermore, information regarding the openings of new vents was noticed and used here to reconstruct the emplacement of the lava-flow fields. Qualitatively assessed time-lines of the lava emplacement during the 1766–68 and 1845–46 eruptions are created similar to those of the 1947–48 eruption by Thórarinsson (1976). It is important to underline that the flow-lines are approximate, but the best possible from combining the historical sources and our analyses. The flow-lines show dates from the literary sources (Figures 3a and 4a). The solid flow-lines indicate that the historical source provides precise information on the location of the flow front by mentioning place names and/or estimate distances from known locations, hence we are more certain of these emplacements. Whereas the dashed lines indicate greater uncertainty because only vague directions of the lava-flow direction are given (e.g. "19 September 1766: .. and lava-flowed both to the west and east and in the direction of Krakatindur" Thórarinsson, 1976).

Fieldwork and geochemical analyses

During fieldwork August 7–10, 2018 we sampled rock specimens and studied flow morphologies of the lava-flows 1766–68, 1845–46 and 1947–48. Four to five specimens were sampled for each of the three lava-flows representing a range of emplacement ages, ideally from oldest to youngest. The samples were analysed at the mineral laboratory Bureau Veritas Commodities Canada Ltd. by XRF and ICP-MS methods to reveal whole rock and trace elements. Analyses of certified reference materials show the relative deviation from the reference values are less than 1% for the major elements and less than 7% for the trace elements discussed in this project. Repeated analyses of samples demonstrate reproducibility within 1% for the major- and minor elements and within 7% for most trace elements.

Viscosity estimates

Several models predict viscosity of silicate melts as a function of temperature and composition (e.g. Shaw, 1972; Bottinga and Weill, 1972; Giordano *et al.*, 2008; Hack and Thompson, 2011). In this study viscosity estimates have been calculated after the model by Giordano *et al.* (2008). This is a multicomponent chemical model spanning most of the compositional range found in natural-existing volcanic rocks. It is based on experimental measurements of viscosity at different temperatures of known melt compositions at atmospheric pressure (10^5 Pa) (Giordano *et al.*, 2008). They use the Vogel-Fulcher-Tammann equation (Vogel, 1921; Fulcher, 1925) to estimate the temperature and composition dependent viscosity (η):

$$log\ \eta = A + \frac{B}{T(K) - C} \quad (1)$$

2. mynd. – *Mynd af hraunþykktarmælingum með dæmum um hæðarsnið B), C), D) og E) ásamt upplýsingum um það hvort mælingarnar uppfylli kröfur sem gerðar voru. Hraunþykktarmælingarnar eru merktar með "accepted" (samþykkt) eða "not accepted" (ósamþykkt) neðst til vinstri á hæðarsniðunum. Hæð við botn hraunsins er merkt með "level 0" (stig 0). Gert er ráð fyrir að þykkt hraunsins sé náð þar sem bratti hraunsins er orðinn lítill. Þetta er táknað með " level 1" (stig 1). Mismunur á hæð stigs 1 og stigs 0 er þykkt hraunsins fyrir það tiltekna snið. Meðalþykkt er áætluð út frá viðurkenndum hæðarsniðum og er notuð í rúmmálsútreikningum. F) Kort af hraunbreiðum frá 1845–46, skipt niður í níu svæði. Nærmyndin sýnir þykktarmælingar (svartar línur). Svæði 1: Gígasvæði og Hekluhryggurinn (halli svæðis er um það bil ≤55°). Svæði 2: flókin formgerð breytist í hraunrás (≤40°). Svæði 3: hraunfossar (≤40°). Svæði 4: hraunflæði í hraunrásum (≤15°). Svæði 5 og 6: mikil hraunbelging og undanrennsli kviku, greinilegast á svæði 5 (≤15°). Svæði 7 og 9: undanrennsli (≤10°). Svæði 8: hraunflæði í hraunrásum, hugsanlega hraunbelging og undanrennsli (≤10°). Bakgrunnur og útlínur eins og á 1. mynd.*

A, B and C are adjustable parameters, though A is assumed to be a constant (see Giordano *et al.* (2008) for arguments therein), which implies that the compositional controls are merely on B and C. The melt temperature is estimated from the relationship between melting temperature and MgO content based on the experimental work on evolved ferrobasalt by Thy *et al.* (2006). Dissolved volatiles like water play a great role in influencing melt viscosity. Since the sampled whole rock are partly or fully degassed, we estimate the primary, pre-eruptive water content from the K_2O-H_2O relationship similar to Lucic *et al.* (2016). It has been shown that H_2O and highly incompatible elements, like K_2O, correlate positively in primary, undegassed melt inclusion of primocryst minerals of Hekla eruptions (Portnyagin *et al.*, 2012; Lucic *et al.*, 2016). The study of Lucic *et al.* (2016) focussed on the volatile compositions of four Hekla eruptions: H3, 1104, 1845 and 1991, which represents a range in repose periods, compositions and volumes of erupted material. They found that H_2O/K_2O ratio of the melt inclusions varied, and generally displayed lower H_2O/K_2O ratio of < 2 as opposed to what have been suggested by earlier studies (e.g. Portnyagin *et al.*, 2012). This suggested loss of water through degassing. The H_2O content representative of degassed magma is measured from glass rims on separated feldspars from basaltic andesite samples of the 2000 Hekla eruption by Höskuldsson *et al.* (2007).

RESULTS

The 1766–68 eruption

The following account is based on the eyewitness description of Finnsen (1767) and Thórarinsson (1967) together with this study's observed lava morphologies and vent structures on the Hekla ridge in the aerial photographs from 1945–46. In the morning of April 5, 1766 Hekla awoke with rumbles and earth tremors and spew "fire, pumice and stones" from the volcano (vent opening not specified). Descriptions of the first days of the eruption focus mainly on the tephra fall and on fluctuations of explosiveness. Two craters were active from the initial phase of the eruption (denoted April 5, 1766–?): the middle crater (more to the SW) on the summit (Figure 3b pink outline) and the crater on the SW shoulder of the Hekla ridge called Bjallagígur that is surrounded by a horseshoe shaped scoria ridge called Höskuldsbjalli (Figure 3b red outline). There are vague descriptions of a third crater also active from the initial phase of the eruption, however, this crater has more likely developed into the ca. 6 km long fissure during the initial phase (Figure 3b purple dashed outline). All three craters were main lava sources for the lavas flowing S-SW (Figure 3a orange outline and yellow dashed outline). However, the two first craters (Figure 3b pink outline and purple dashed outline) were mainly active during the first days of the eruption and Bjallagígur was active during the whole of the eruption. Mentions of at least seven craters near the main three craters at the mid to the SW shoulder of the ridge are given. We interpret these observations as if they were part of the fissure opening (Figure 3b purple dashed outline) as we could not detect them on the aerial orthophotos. Moreover, outpouring of lava has likely drowned some of the fissure and later modifications from the 1845–46 eruption as well as subsequent erosion has changed the summit ridge. The first description of lava outpouring is on April 9. Lava was seen flowing towards SSW stretching as far as the north end of Vatnafjöll with a length of about 7 km (Figure 3a orange outline). On April 15–21, a great flow of lava emerged resulting in a flow field extending to the SW (Figure 3a yellow

3. mynd. – *Kort sem sýnir líklegt hraunflæði í gosinu 1766–68, byggt á sögulegum heimildum. Heilar línur sýna útbreiðslu hraunflákanna, byggða á nákvæmum lýsingum. Brotalínur tákna áætlaða útbreiðslu hraunflákanna. Bakgrunnur kortsins er sá sami og á 1. mynd. B) Nærmynd af Hekluhryggnum sýnir að minnsta kosti fimm gígar voru virkir á árunum 1766–68. Loftmyndin er frá 1945–46, þá hafði Hekluhryggurinn þegar breyst eftir gosin 1766–68 og 1845–46, og vegna rofs sem varð í kjölfar þeirra. Heilar línur tákna gíga sem nokkuð öruggt er að hafi verið virkir á þessum tíma, og brotalínur ógreinilegri gíga á loftmyndinni. Túlkun þessi er eingöngu byggð á rituðum heimildum.*

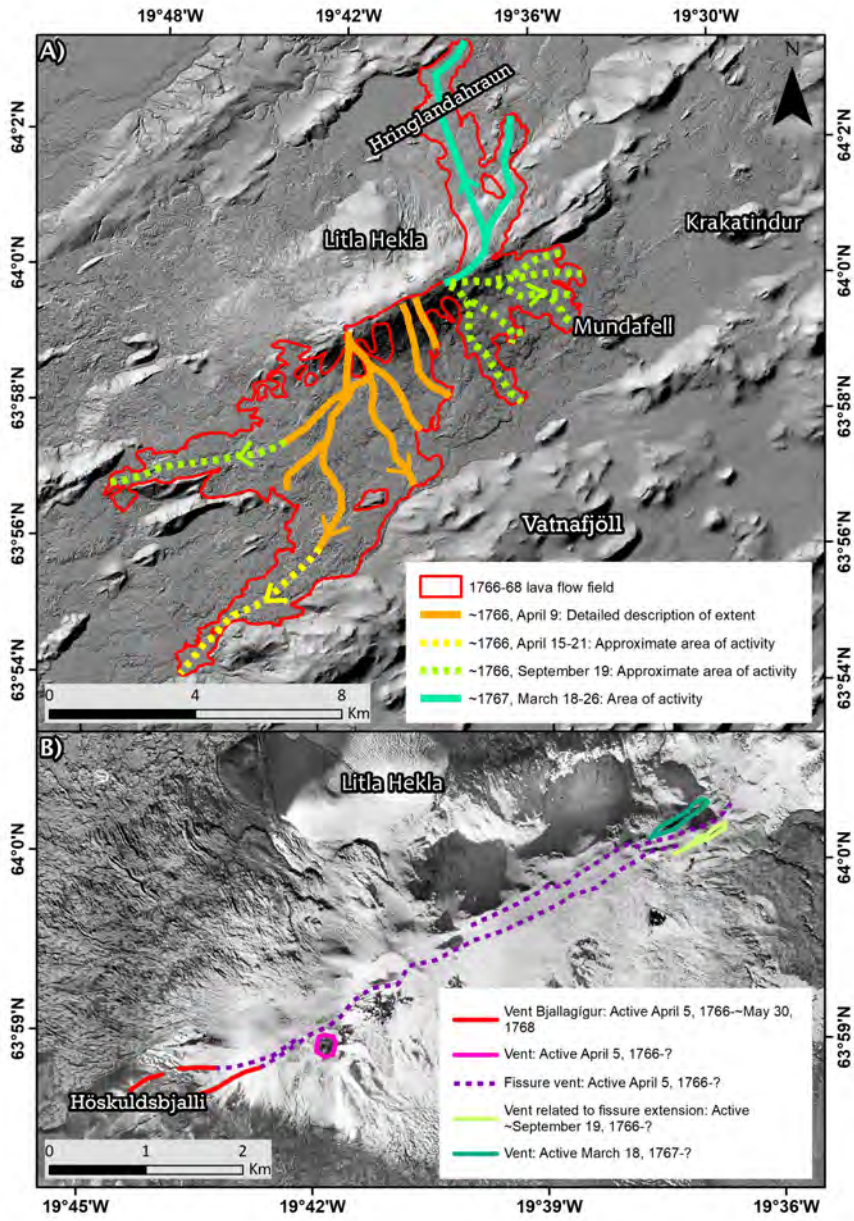

Figure 3. A) Lava-flow-line chart of the 1766–68 eruption based on descriptions from historical sources. Solid lines indicate that the lava extent is based on precise descriptions. The dashed lines represent approximate lava extent. Background and boundary outlines as in Figure 1. B) Close-up of the Hekla ridge pinpointing at least five active craters during 1766–68. The orthophoto is from 1945-46, thus the Hekla ridge had already been modified since the 1766–68 eruption by the 1845–46 eruption and subsequent erosion. Solid lines mark greater certainty of active craters and the dashed lines mark uncertainty due to indistinct vents in the orthophoto, i.e. these interpretations are based on the literary descriptions alone.

dashed outline). Mentions of lava were once again noted on September 19, where lava flowed both to the west and to the east in the direction of Krakatindur (Figure 3a green dashed outline). The eruptive activity in general is described as being variable between April 9 and September 19 with explosive activity and earth tremors. It is therefore likely that an extension of the vent opening of the Hekla ridge and possibly new vent openings related to the larger vent extension to the NE may explain how the lava could flow towards Krakatindur (Figure 3b purple dashed outline and solid light-green outline). The lavas that flowed generally towards S-SW from the Hekla ridge display complex morphology, e.g. lava-flows resembling arteries which are signs of vertical stacking of numerous surges of lava. In addition, inflation structures are prominent, implying stalling of lava, and (often) in connection to breakout structures. It appears from the aerial orthophotos that there are at least two types of breakout structures representing two flow rates. One type looks thinner and smoother, slightly similar to the sheet-like-flows observed. The second type lavas look bulky and have not flowed as far unlike the aforementioned type. The literary sources from Thórarinsson (1967) and Einarsson (1949) mention a "lava flood"-type and a "toothpaste-tongue"-type, respectively, thus there is a consistency between the observations of the aerial orthophotos and the literary sources of two different types of breakouts. The lava-flow towards E in the direction of Krakatindur is a sheet-like-flow (Figure 3a green dashed outline E from Hekla ridge), thus, in contrast to the main lava-outpouring to the S-SW of the Hekla ridge, this lobe likely represents a single surge of lava. In the beginning of the year 1767 Hekla seemed to "loose its breath" with the whole of February being quiet. On March 18, 1767, a large eruption began again with detonations, an eruption column, some ash fall, and rapid lava-flow flowing to the North (the lava-flow called Hringlandahraun) until March 26 (Figure 3a turquoise solid outline). This suggests that a new vent (or vents) became active on the north-eastern part of the summit ridge (Figure 3b green outline). Similar to the lava flowing towards Krakatindur, the Hringlandahraun is a sheet-like-flow, thus representing a faster, single surge of lava. Hereafter, there are no descriptions of lava activity. From April 1 to June 1, 1767, Hekla's activity is described as fluctuating in regard to its explosiveness, emission of ash, fire and smoke. Hekla was quiet the whole month of June. In July and August little activity in the form of ash and smoke emerged. After August and the remainder of 1767, Hekla was quiet. In March and April 1768 "Hekla seemed to wish to waken from its slumber again". Smoke and fire were observed by people on May 11 and 30. Following May 30, 1768, the eruption ended.

The detailing of the effusive activity is rather sparse, therefore, few dates of lava emplacement can be deduced and outlined on the map (Figure 3a). Detailed description of the southern lava flow field exists for April 9, while further deduction of extent is uncertain. We are certain that the descriptions of new increased explosive activity resulting in new vent openings on the north-eastern side of the Hekla ridge on ca. March 18, 1767 resulted in the emplacement of the Hringlandahraun lava field (Figure 3a turquoise solid outline), because the previously described vents are unable to emplace lava at that location. Furthermore, the observed morphology of Hringlandahraun is a sheet-like-flow, which fits the description of rapid lava emplacement. Thus, the Hringlandahraun was emplaced at or after March 18, 1767, implying it is younger than the lava field to the S-SW and E of the Hekla ridge.

The entire area of the exposed flow field is 49.8 km^2. For the planimetric method, 44 thickness profiles were measured along the lava fronts and unevenly distributed indifferent to the nine zone divisions. The estimated flow thicknesses vary from 5.3–22.8 m and the average thickness for the entire flow is 13.7 m. The estimated bulk volume is 0.7 km^3.

The 1845–46 eruption

The following account is based on the description of Schythe (1847) and Thórarinsson (1967). After a repose period of 77 years, Hekla showed activity again on September 2, 1845. The opening phase was plinian, lasted approximately one hour and produced 7.5×10^{10} kg and 0.13 km^3 tephra deposited from a 19 km high eruption plume to the ESE of Hekla (Gudnason *et al.*, 2018). Following the plinian phase, both

tephra and lava erupted. Lava emission on the first day was described as being very large and flowing swiftly. In the beginning (September 2, 1845), lava mainly erupted from the central crater and the crater on the SW shoulder of the Hekla ridge (Figure 4b green and turquoise outlines). Additionally, three craters are reported locating closely together (forming a fissure) next to the crater on the SW shoulder of the ridge (Figure 4b dark red dashed outline). The smallest, lowest and south-westernmost on the ridge of the three craters is considered the main source of the 1845–46 eruption, and from which the youngest 1845–46 lava erupted. It is, however, not clear when the smallest crater took over the main activity, but it is certain that all five craters were active from the beginning of September 2, 1845. The lava flowed mainly W and NW in the direction of the Melfell ridge and towards the old Næfurholt farm (Figure 4a). The morphology is mainly characterised by channelised flows in the central area of the flow field and vertical stacking of lavas closest the Hekla ridge. On September 9, the lava fronts were nearly 2 km east of Melfell (Figure 4a orange outlines). On September 12, the lava-flow began to advance westwards on both sides of Melfell (Figure 4a red outlines). On September 21, the lava was described having advanced 183 m further westwards between Melfell and Markhlíð (Figure 4a light-pink outline) and in the following two days the people residing at the Næfurholt farm fled because the lava cut off their water supply, and they feared that the lava would bury their farm. However, at about that time the lava is described having changed its course to flow towards NNW on the east side of Melfell (Figure 4a light-pink dashed outline). Thus the lavas stalled and resulted in inflation structures visible on the aerial orthophotos. In general, inflation structures are observed at flow margins and in connection with breakout structures, e.g. the lava flowing between Melfell and Markhlíð is the result of a breakout (Figure 4a light-pink and dark-purple solid outlines). In some areas (e.g. NW of Litla Hekla) the breakouts somewhat resembles cauliflowers (maybe faster-flowing breakout?). On October 18, a new, small lava-flow began at the summit ridge crater, or as a breakout from the main existing lava stream, and flowed SW in the direction of a place later called Þrætustígur (Figure 4a dark-pink outline). On November 14, the main lava-flow field (and breakout) had completely encircled Melfell (Figure 4a dark-purple outline), and on November 19 it had flowed down into the gully nearest the Næfurholt farmstead. The lava stopped at its maximum length of ca. 10 km from the summit ridge on November 25 having passed close by the Næfurholt farmstead (Figure 4a blue outline). After November 25 and to the end of November, the eruption apparently paused. After this approximately month long pause, lava activity is reported (unclearly) occurring on December 27, 1845, January 26-February 5, 1846 and March 3–16, 1846 mainly with lava emission flowing towards N-NW, passing Litla Hekla on its west side (Figure 4a green dashed outlines). Thórarinsson (1967) reports pauses in the lava emission and the explosive activity in the periods November 17-30, 1845 and January 25 to March 2 and March 23-24, 1846 which contradicts the above mentioned dates of lava activity, thus it is uncertain when the pauses occurred, and what the pauses exactly mean. The 1845–46 eruption ended April 5–10, 1846. A possible small recurrence in the form of a dense cloud rising from the volcano emerged August 13–16, 1846.

The entire area of the flow field is 24.8 km^2. The area of the nine zones and their average thickness (measure by a total of 37 thickness profiles) reveal thicknesses from 4.4–28.1 m (Figure 2f). The estimated bulk volume is 0.4 km^3, and the average thickness for the entire flow field is 14.7 m.

Bulk rock compositions and viscosity

This study's samples have an average MgO content of 2.55 wt% which corresponds to a melting temperature of 1060°C according to Thy *et al.* (2006). Hence, we apply the temperature 1060°C in the Giordano *et al.* (2008) model. Our samples are mostly basaltic andesite with 54–58 wt% SiO_2 (Table 2), and the two eruptions 1766–68 and 1845–46 demonstrate similar trends of MgO decreasing and K_2O increasing respectively with increasing SiO_2 (Figure 5a, b). These compositions are comparable to the 1991 Hekla samples from Lucic *et al.* (2016). Hence, pre-eruption H_2O of our samples can be estimated assum-

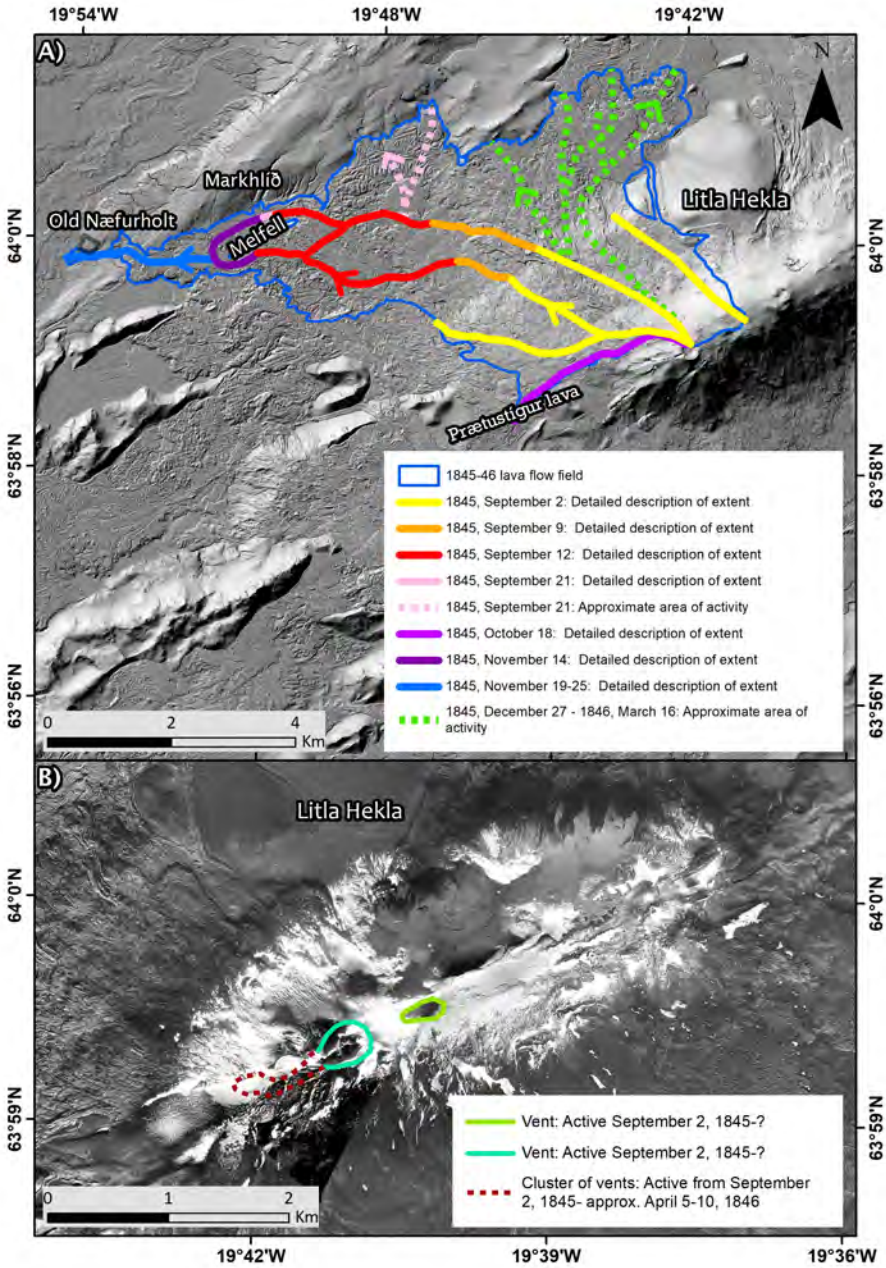

Figure 4. A) Lava-flow-line chart of the 1845–46 eruption based on descriptions from historical sources. Solid lines indicate that the lava extent is based on precise descriptions. The dashed lines represent approximate lava extent. Background and boundary outlines as in Figure 1. B) Close-up of the Hekla ridge pinpointing active craters during 1845–46. The orthophoto is from 1945–46. Solid lines mark greater certainty of active craters and the dashed lines mark uncertainty due to indistinctly vents in the orthophoto.

4. mynd. – *Þróun útbreiðslu hraunflákanna frá 1845–46 byggð á sögulegum heimildum. Heilar línur sýna útbreiðslu hraunflákanna byggða á nákvæmum lýsingum. Brotalínur tákna áætlaða útbreiðslu hraunflóða. Bakgrunnur kortsins er sá sami og á 1. mynd. B) Nærmynd af Hekluhryggnum, virkir gígar á árunum 1845–46 eru merktir á kortið. Loftmyndin er frá 1945–46. Heilar línur tákna virka gíga og brotalínur ógreinilegri gíga á loftmyndinni.*

Table 2. Whole rock analysis and viscosity estimates of the Hekla rock samples from the 1766–68 and 1845–46 lava-flows. Viscosity is estimated by means of the model by Giordano *et al.* (2008), emplacement time/period of the samples are based on the historical sources (see text), and the morphology surface structures are based on observations from the field and orthophotos. – *Efnagreiningar og mat á seigju sýna frá hraununum sem runnu 1766–68 og 1845–46. Seigjan er áætluð út frá líkani Giordano o.fl. (2008) og aldur sýnanna er byggður á sögulegum gögnum (sjá texta). Formgerð sýnanna er byggð á rannsóknum í felti og loftmyndum.*

Eruption		1766–68					1845–46				
Approximate emplacement date		April 9–21, 1766	Sept. 9, 1766	Sept. 9, 1766	Sept. 9, 1766	March 18, 1767	Sept. 12, 1845	Nov. 14, 1845	Nov. 14, 1845	Nov. 19–25, 1845	Dec. 27, 1845–March 16, 1846
Sample no.		**18IS-21**	**18IS-07**	**18IS-08**	**18IS-09**	**18IS-16**	**18IS-05**	**18IS-02**	**18IS-03**	**18IS-06**	**18IS-15**
Morphology		Complex	Inflation		Bulky breakout	Sheet-like flow	Inflation	Channelised flow	Smooth breakout	Channelised flow	Smooth breakout
SiO_2	(wt%)	54.90	56.50	56.40	56.40	57.80	57.10	55.20	56.50	54.70	54.00
Al_2O_3	(wt%)	14.80	15.00	15.00	15.00	15.20	15.10	14.90	15.00	14.80	14.70
Fe_2O_3	(wt%)	13.00	11.80	11.90	11.90	11.20	11.50	12.80	11.40	12.90	13.50
FeO	(wt%)	5.85	5.31	5.35	5.35	5.04	5.17	5.76	5.13	5.80	6.07
FeO^T	(wt%)	17.54	15.92	16.05	16.05	15.11	15.51	17.27	15.38	17.40	18.21
CaO	(wt%)	6.64	6.15	6.15	6.16	5.77	6.00	6.52	5.93	6.62	6.91
MgO	(wt%)	2.82	2.43	2.43	2.42	2.15	2.34	2.73	2.31	2.80	3.04
Na_2O	(wt%)	4.16	4.33	4.29	4.32	4.41	4.35	4.26	4.29	4.18	4.07
K_2O	(wt%)	1.26	1.36	1.36	1.36	1.45	1.41	1.30	1.39	1.27	1.20
MnO	(wt%)	0.29	0.27	0.27	0.27	0.26	0.27	0.29	0.26	0.29	0.30
TiO_2	(wt%)	1.92	1.65	1.65	1.65	1.46	1.58	1.86	1.56	1.91	2.08
P_2O_5	(wt%)	1.03	0.83	0.83	0.83	0.70	0.78	0.99	0.77	1.02	1.16
H_2O	(wt%)	1.24	1.34	1.34	1.34	1.43	1.39	1.28	1.37	1.25	1.18
Viscosity											
Pre-eruption 1060°	log η (Pa s)	2.26	2.41	2.40	2.39	2.49	2.44	2.27	2.45	2.25	2.19
	η (Pa s)	180.29	254.44	248.91	247.66	311.50	276.50	184.39	281.06	178.57	155.12
Degassed 1060°	log η (Pa s)	3.15	3.40	3.39	3.38	3.56	3.47	3.19	3.47	3.15	3.04
	η (Pa s)	1419.27	2500.54	2429.23	2415.85	3638.89	2963.15	1539.00	2955.40	1423.23	1091.63

Viscosity estimated by the VTF equation: log η (Pa s) = A + B/[T(K)-C] and model coefficients see Giordano *et al.* (2008). Pre-eruptive water content estimated from the H_2O/K_2O relationship from the 1991 samples by Lucic *et al.* (2016). Degassed magma water content from Höskuldsson *et al.* (2007). – *Seigjan er áætluð með VTF jöfnunni: log η (Pa s) = A + B / [T (K) -C] og líkanstuðlarnir eru frá Giordano o.fl. (2008). Vatnsinnihald fyrir gos er áætlað út frá H_2O / K_2O hlutfalli úr sýnum frá 1991 eftir Lucic o.fl. (2016). Afgasað kvikuvatnsinnihald er frá Höskuldssyni o.fl. (2007).*

ing H_2O/K_2O of 0.98 following the relationship from Lucic *et al.* (2016) for the average of the 1991 samples. This results in an average of 1.3 wt% H_2O in our samples (Table 2). Based on these assumptions the estimates of pre-eruptive melt viscosity ranges from 1.8×10^2 – 3.1×10^2 Pa s (1060°C) for the 1766–68 lava-flows, and 1.6×10^2 – 2.8×10^2 Pa s (1060°C) for the 1845–46 lava-flows (Table 2). The whole rock data of our samples are also comparable to the 2000 Hekla samples from Höskuldsson *et al.* (2007) from which they measured 0.14 wt% water at a corresponding liquidus temperature of 1136°C as the component representative of degassed magma. To estimate the viscosity of degassed magma represented by our samples we apply this H_2O content of 0.14 wt% (Table 2). This results in melt viscosity ranges of 1.4×10^3 – 3.6×10^3 Pa s (1060°C) for the 1766–68 lava-flows, and 1.1×10^3 – 2.9×10^3 Pa s (1060°C) for the 1845–46 lava-flows (Table 2). Our viscosity results show one order of magnitude difference between unde-

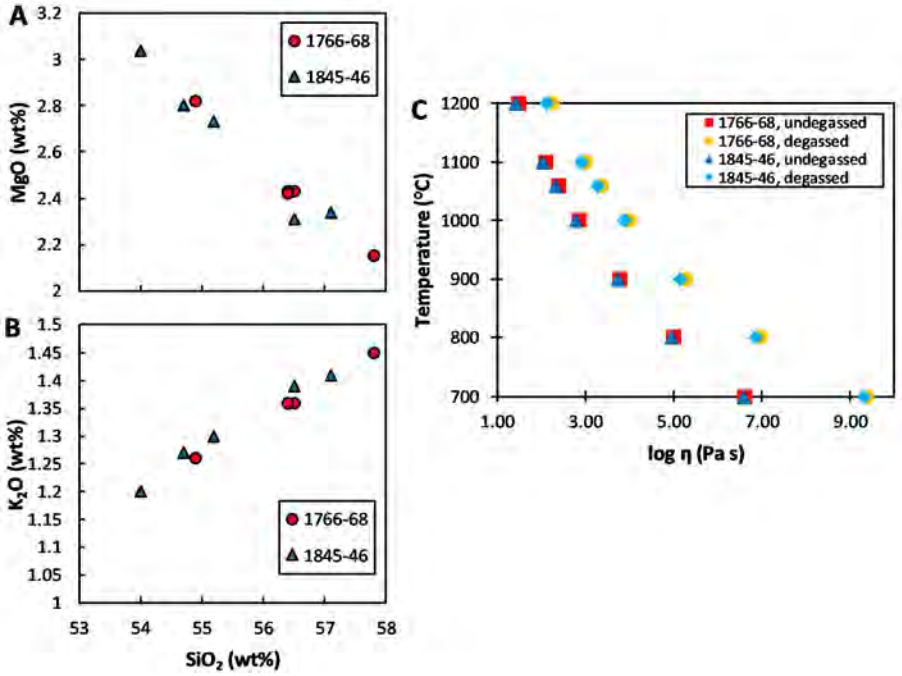

Figure 5. Whole rock and viscosity estimates of the Hekla 1766–68 and 1845–46 samples analysed in this study. Panels show A) MgO and B) K_2O versus SiO_2 content, and C) our viscosity estimates versus temperature for respectively pre-eruptive (undegassed) and degassed melts. – *Efnagreiningar og mat á seigju Heklusýnanna frá hraunbreiðunum 1766–68 og 1845–46. Myndirnar sýna A) MgO, B) K_2O samanborið við SiO_2 innihald og C) Mat á seigju miðað við hitastig kvikunnar áður en hún gaus og eftir (afgösuð kvika).*

gassed and degassed magma. Emplacement dates and morphology surface structures related to the sampled lava-flows are listed together with the samples' bulk rock composition and viscosity estimates (Table 2).

DISCUSSION

Lava bulk volumes and accuracy of the planimetric method

New volume estimates for the 1766–68 and 1845–46 lava-flow fields are provided. Thórarinsson (1967) previously estimated the volume to 1.3 km^3 and 0.6 km^3, respectively, but the basis of these estimates remains unclear (e.g. method of thickness estimates and the number and location of measurements). In contrast the bulk volume estimates of this study gives volumes of 0.7 km^3 (47% smaller) and 0.4 km^3 (42% smaller), respectively. Because of the inherent errors connected with the assumptions of the planimetric method (e.g. the limitation of thickness estimates to the lava margins), it is impossible to estimate an error. However, it is possible to get an idea of the accuracy by comparing the volume estimates for the 1947–48 lavas calculated with the planimetric method with the volume estimates from Pedersen *et al.* (2018a). They made accurate lava-flow thickness maps for the 20th century lava-flows by differencing pre- and post-eruption DEMs generated from historical stereo photographs. The planimetric method yields for the 1947–48 lava-flow field a volume estimate of 0.4 km^3, which is 44% lower compared to the volume result of 0.742 ± 0.138 km^3 by Pedersen *et al.* (2018a). Likewise, Montalvo (2013) provided a volume estimate of 0.07 km^3 for the 1980-81 lava-flow field using the planimetric method, which is nearly 60% smaller than the estimated 0.169 ± 0.016 km^3 by

Pedersen *et al.* (2018a). This suggests that the planimetric method may underestimate the lava bulk volume in the order of 40-60%. Wadge (1978) similarly estimated that the planimetric method may underestimate volumes by approximately 50%. Thus, considering this, it is likely that the volume of the 1845–46 is 0.5–0.6 km^3 and 1766–68 may be 1.0–1.2 km^3. Taking this into account, the estimates thus confirms the estimates provided by Thórarinsson (1967).

The production rate, which is defined as erupted material in an eruption divided by pre-eruption repose period, varied from 7.4×10^6 to 40×10^6 m^3yr^{-1} for the Hekla eruptions during the 20th century (Pedersen *et al.*, 2018a). Our data yields production rates of 15×10^6 m^3yr^{-1} and 7.2×10^6 m^3yr^{-1} for the 1766–68 (repose period of 73 years) and 1845–46 (repose period of 77 years) eruptions, respectively. Pedersen *et al.* (2018a) stated that production rates at Hekla are variable on 10–100 year time scale in contrast to a steady production rate which was proposed earlier (see references therein). Our production rates respectively for the 1766–68 and 1845–46 agree with the statement from Pedersen *et al.* (2018a).

Viscosity estimates

Viscosity estimates showed that pre-eruptive magmas (2.5×10^2 Pa s and 2.2×10^2 Pa s in average for 1766–68 and 1845–46 eruptions, respectively) were about one order of magnitude more fluid than the degassed magmas (2.5×10^3 Pa s and 1.9×10^3 Pa s in average for 1766–68 and 1845–46 eruptions, respectively). In addition to water, decreasing temperature accelerates the increase in viscosity exponentially (Figure 5c). Lowering the temperature has the effect of accelerating the increase of viscosity by one to two orders of magnitude (Figure 5c). We expect a large range in the viscosity of lava during emplacement, resulting in variable shear strain rates and resulting surface crust structures (Pedersen *et al.*, 2017). Similarly, Kolzenburg *et al.* (2017) showed that viscosity can increase 3 orders of magnitude during the eruption of Holuhraun. From field observations and studying the orthophotos the sampled lava-flows are from inflation structures (18IS-05, -07 and -08), complex morphology (18IS-21), channelised flow (18IS-02 and -06), sheet-like-flow (18IS-16), bulky type of breakout structures (18IS-09) and smooth type of breakout structures (18IS-03 and -15). There is not a simple relationship between the estimated viscosities for the samples and the observed flow morphologies (Table 2). This is most likely due to the large variation in viscosity due to variable degassing, cooling and crystallisation during emplacement. We can therefore not assume that our estimates fully capture the entire span of viscosity for the Hekla lavas during the 1766–68 and 1845–46 eruptions, since this would require actual emplacement temperature and actual crystal content measurements.

Combining Hekla's emplacement time-lines and SiO_2 contents

Several models of the magma reservoir beneath Hekla's central volcano have been suggested to explain the chemically-zoned tephra deposits. Hekla tephras typically change from silicic (white) of rhyolite composition at the base grading upwards to andesite composition (black) at the top, followed by lavas of the composition andesite (ca. 58 wt% SiO_2) to basaltic andesite (54 wt% SiO_2) as typical end composition (Sigmarsson *et al.*, 1992; Sverrisdottir, 2007; Chekol *et al.*, 2011; Janebo *et al.*, 2018). This has been explained by a stratified magma chamber model with the most SiO_2 rich magmas at the top. This popular model was first proposed by Sigmarsson *et al.* (1992) and has been slightly modified by Sverrisdottir (2007) and Chekol *et al.* (2011). Thus, the tapping of such a stratified plumbing system starts with the most silica-rich magmas (rhyolite) during the initial explosive phase (Thórarinsson, 1967; Sigmarsson *et al.*, 1992; Sverrisdottir, 2007; Janebo *et al.*, 2016b). The SiO_2 content of the later tephras and lavas decline to andesite and basaltic andesite (Sigmarsson *et al.*, 1992; Sverrisdottir, 2007). Therefore, it is to be expected that the silica content of the large lava-flow fields will also follow this pattern, showing a decline of SiO_2 over time. Our data enables us to test this hypothesis by comparing the emplacement time-lines with the SiO_2 of the samples (Table 2). For the 1845–46 and 1947–48 eruptions, the SiO_2 evolution is indeed decreasing with time, supporting the stratified magma chamber model (Figure 6b, c). In these cases, the SiO_2 contents of the studied samples

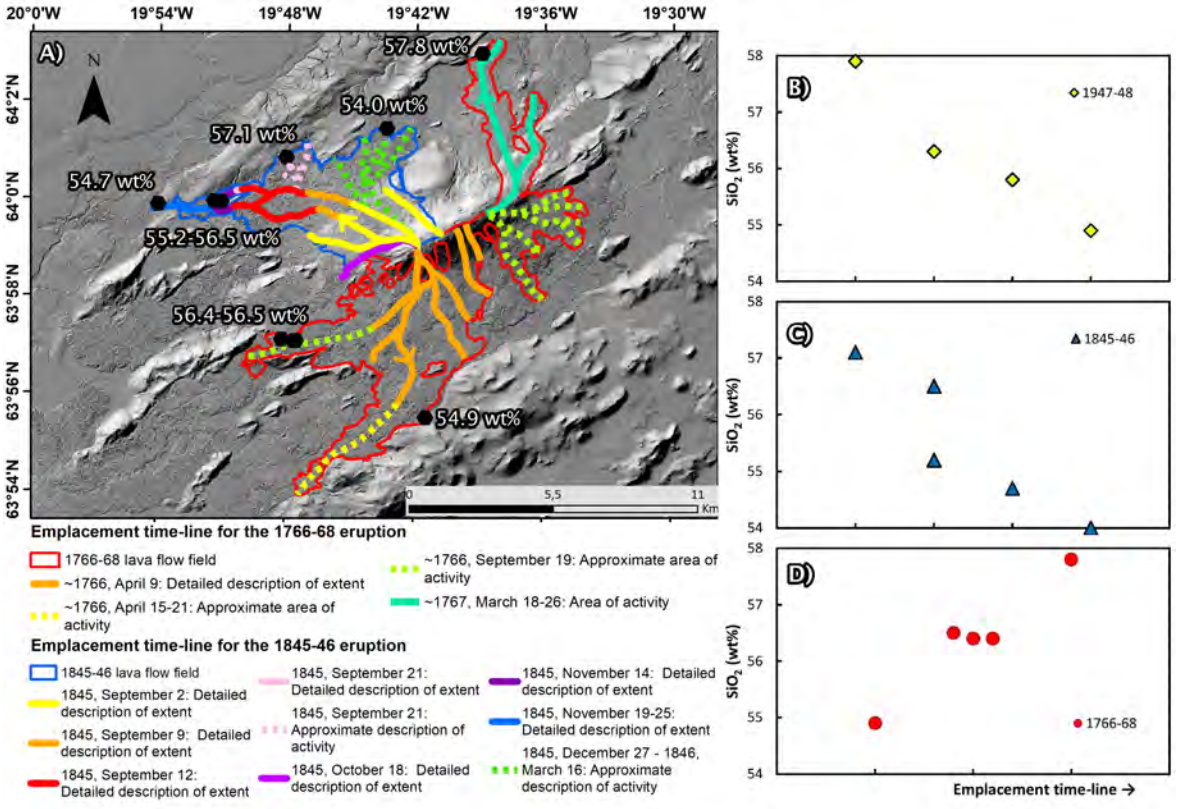

Figure 6. A) Lava-flow-lines of the 1766–68 and 1845–46 eruption (explanations given in Figures 3 and 4 are applicable here) combined with sample location and SiO_2 wt% content (Table 2). Background and boundary outlines as in Figure 1. B), C) and D) are panels showing SiO_2 of the lava samples versus their emplacement ages respectively for the 1947–48, 1845–46 and 1766–68 eruptions. Sample points placed from older to youngest lavas towards the right on the x-axis. – *Þróun útbreiðslu hraunflákanna árin 1766–1768 og 1845–46 (sjá skýringatexta á myndum 3 og 4), ásamt staðsetningu sýnatökustaða og SiO_2 hlutfalli í sýnum (tafla 2). Bakgrunnur kortsins er sá sami og á 1. mynd. B), C) og D) sýna SiO_2 hlutfall í sýnunum miðað við aldur þeirra, sýnin eru frá eldgosunum 1947–48, 1845–46 og 1766–68. Elstu sýnin eru vinstra megin og þau yngstu hægra megin.*

change from ca. 57 to 54 wt% and ca. 58 to 55 wt%, respectively. The 1766–68 eruption is more complicated than such. Mainly one sample (18IS-16) from the northern Hringlandahraun flow field differs from the expected trend of a secular SiO_2 decline (Figure 6a, d). This sample from the front of Hringlandahraun flow field has higher SiO_2 content (57.8 wt%) compared to the samples from the southern lava-flows (54.9-56.5 wt%) (Figure 6a). As described above, Hringlandahraun erupted from the NE vent that was active from March 18, 1767 (Figure 3a, b), thus originated from a later opening compared to the southern lava-flow that emanated from craters active from the beginning of the eruption (April 5, 1766). We do not know if the sample from Hringlandahraun indicates that the SiO_2 content of the 1766–68 increased during the eruption or if the SiO_2 content fluctuated. Nonetheless, we are certain of the emplacement period of Hringlandahraun, because there are only descriptions mentioning intense flow of lava to the north

after the new vent opening at March 18, 1767, and the observed lava-flow morphology from the aerial orthophotos confirms these descriptions (Figure 3a, b). Therefore, the high-SiO_2 lavas of Hringlandahraun was emplaced late in the eruption. This discovery challenges the conventional model of tapping of a single, large, layered magma chamber with the most evolved (silica-rich) magmas at the top. The simplest explanation is that the NE end of the summit ridge, at least in 1766–68, tapped a different source, but this should be investigated further requiring more detailed sampling of the different phases of the eruptions. However, based on our results the eruption of the 1766–68 lava-flows are inconsistent with a single, stratified magma chamber model from which the erupted products become poorer in SiO_2 with time.

CONCLUSIONS

The estimated bulk volume based on the planimetric method for the 1766–68 Hekla eruption is 0.7 km^3 and for the 1845–46 eruption is 0.4 km^3. Based on volume comparisons between the planimetric method and digital elevation model (DEM) thickness maps for the 1947–48 eruption, it is suggested that the planimetric method may underestimate the lava bulk volume by 40–60%. Hence, the true bulk volumes of the 1766–68 and 1845–46 eruptions are more likely 1.0–1.2 km^3 and 0.5–0.6 km^3, respectively. We estimate viscosities representative of pre-eruptive (average 1.3 wt% H_2O) and degassed magmas (0.14 wt% H_2O). The undegassed melt viscosity ranges from 1.8×10^2–3.1×10^2 Pa s (1060°C) for the 1766–68 lava-flows, and 1.6×10^2–2.8×10^2 Pa s (1060°C) for the 1845–46 lava-flows, and the degassed melt viscosity ranges from 1.4×10^3–3.6×10^3 Pa s (1060°C) for the 1766–68 lava-flows, and 1.1×10^3–2.9×10^3 Pa s (1060°C) for the 1845–46 lava-flows. This presents one order of magnitude difference between pre-eruptive and degassed magma, and confirms that the pre-eruptive magma is more fluid than the degassed magma. The emplacement time-lines of the lavas combined with the silica content of collected samples show that SiO_2 decreased from ca. 58 to 54 wt% during eruptions in 1845–46 and 1947–48. In contrast, our results from the 1766–68 eruption suggest that SiO_2 fluctuated increasing from ca. 55 to 58 wt% during the emplacement of Hringlandahraun, revealing that not all Hekla eruptions necessarily follow a decline in SiO_2 during the eruption. This implies that the model assuming magma being tapped successively from the top of a stratified magma chamber may not be applicable to all Hekla eruptions.

ACKNOWLEDGEMENTS

We would like to acknowledge the Icelandic Research fund, Grant of Excellence No. 152266-052 (Project EMMIRS) for supporting the field trip and access to the remote sensing data. This research was also funded by the Danish National Research Foundation Niels Bohr Professorship grant 26-123/8. Thanks to Landgræðsla ríksins for their help during fieldwork. The first author also acknowledges Selskabet Arktisk Forskning og Teknologi (SAFT) for funding of travels connected to this project. Extended thanks go to editor Bryndís Brandsdóttir and two anonymous reviewers for their thorough and constructive reviews. Lastly, thanks to Páll Einarsson for help with the Icelandic translation of the abstract and for proof-reading the manuscript. Also thanks to Stefán Már Melstað for help with the Icelandic abstract and to Ásta Rut Hjartardóttir for help with the Icelandic translation of the figure- and table texts.

Ágrip

Rúmmál hrauna sem runnu í Heklugosunum 1845–1846 og 1766–1768 er endurmetið út frá nýjum fjarkönnunargögnum, sögulegum heimildum, bergfræði og seigju hraunanna, sem reikna má út frá efnasamsetningu þeirra. Ef reiknað er út frá flatarmáli hraunanna og ætlaðri þykkt þeirra fæst rúmmál 0,4 km^3 og 0,7 km^3 fyrir gosin tvö. Ef sömu aðferð er beitt á gosið 1947 kemur í ljós að hún vanmetur rúmmálið um 40–60%. Því eru rúmmál eldgosanna 1845–46 og 1766–68 áætlað 0,5–0,6 km^3 og 1,0–1,2 km^3. Við áætlum seigju kvikunnar út frá efnasamsetningu og gasinnihaldi. Ætla má að seigja kvikunnar fyrir gosið 1766–1768 hafi verið 2,5 x 10^2 Pa s en 2,5 x 10^3 Pa s eftir að gasið rauk úr henni. Fyrir gosið 1845–1846 er seigja kvikunnar metin 2,2 x 10^2 Pa s en eftir að gasið rauk úr er hún metin 1,9 x 10^3 Pa s. Seigja kvikunnar vex nær tífalt þegar hún gýs og losar sig

við gasið. Nota má söguleigar heimildir og fjarkönnunargögn til að ákvarða straumlínur hraunrennslisins og rekja breytingar á gígunum á gossprungu Heklu meðan á gosunum stóð.

Í eldgosunum 1845–46 og 1947–48 minnkaði SiO_2 úr 58–57 wt% í upphafi goss í 55–54 wt% í lok goss. Þetta er í samræmi við hefðbundið líkan um að Hekla gjósi úr einu stóru, lagskiptu kvikuhólfi þar sem mest þróaða (kísilríkasta) kvikan liggur efst. Aftur á móti sýna hraunin frá 1766–68 flóknari SiO_2 þróun. Hraunið frá 1766 frá suðurhluta Heklusprungunnar hafði SiO_2 hlutfall á bilinu 54,9–56,5 wt%, en Hringlandahraunið sem rann síðar frá NE-enda Heklu í mars 1767 hafði hærra hlutfall SiO_2, um 57,8 wt%. Þetta sýnir að einfalda lagskipta kvikuhólfslíkanið fellur ekki að öllum hraungosum Heklu.

REFERENCES

Albino, F., B. Smets, N. d'Oreye and F. Kervyn 2015. High-resolution TanDEM-X DEM: An accurate method to estimate lava flow volumes at Nyamulagira volcano (D. R. Congo). *J. Geophys. Res. Solid Earth* 120, 4189–4207, https://doi.org/10.1002/-2015JB011988.

Barsotti, S., M. M. Parks, M. A. Pfeffer, M. J. Roberts, B. G. Ófeigsson, G. B. Guðmundsson, K. Jónsdóttir, K. Vogfjörð, I. Kristingsson, B. H. Bergsson and R. H. Þrastarson 2019. *Hekla volcano monitoring project.* Icelandic Meteorological Office, Report to ICAO, VÍ 2019-003, 60 pp.

Björnsson, H. 1983. Obituary: Sigurdur Thorarinsson, 1912–1983. *J. Glaciology* 29, 521–523.

Bonny, E., T. Thordarson, R. Wright, A. Höskuldsson and I. Jónsdóttir 2018. The Volume of Lava Erupted During the 2014 to 2015 Eruption at Holuhraun, Iceland: A Comparison Between Satellite- and Ground-Based Measurements. *J. Geophys. Res. Solid Earth* 123, 5412–5426, https://doi.org/10.1029/2017JB015008

Bottinga, Y. and D. F. Weill 1972. The viscosity of magmatic silicate liquids; a model calculation. *Am. J. Science* 272, 438–475, https://doi.org/10.2475/-ajs.272.5.438.

Bricka, C. F. 2019. *Dansk biografisk leksikon* 5, http://-runeberg.org/dbl/15/0414.html, 412 pp.

Calvari, S. and H. Pinkerton 1998. Formation of lava tubes and extensive flow field during the 1991–1993 eruption of Mount Etna. *J. Geophys. Res. Solid Earth* 103, 27291–27301, https://doi.org/10.1029/97JB03388.

Calvari, S. and H. Pinkerton 1999. Lava tube morphology on Etna and evidence for lava flow emplacement mechanisms. *J. Volc. Geoth. Res.* 90, 263–280, https://doi.org/10.1016/S0377-0273(99)00024-4.

Chekol, T. A., K. Kobayashi, T. Yokoyama, C. Sakaguchi and E. Nakamura 2011. Timescales of magma differentiation from basalt to andesite beneath Hekla Volcano, Iceland: Constraints from U-series disequilibria in lavas from the last quarter-millennium flows. *Geochim. Cosmochim. Acta* 75, 256–283, https://doi.org/10.1016/j.gca.2010.10.001.

Einarsson, P. and K. Sæmundsson 1987. Earthquake epicenters 1982–1985 and volcanic systems in Iceland. Map in: *Í hlutarins eðli.* Sigfússon, Þ. I. (ed.). Festschrift for Þorbjörn Sigurgeirsson. Menningarsj., Reykjavík.

Einarsson, P. 2018. Short-term seismic precursors to Icelandic eruptions 1973–2014. *Frontiers in Earth Science* 6, https://doi.org/10.3389/feart.2018.00045.

Einarsson, T. 1949. *The Eruption of Hekla 1947–1948: The flowing lava. Studies of its main physical and chemical properties.* 1–70 pp. Einarson, T., G. Kjartansson and S. Thórarinsson (eds.). The Museum of Natural History, Reykjavík.

Fink, J. 1980. Surface folding and viscosity of rhyolite flows. *Geology* 8, 250–254, https://doi.org/10.1130/-0091-7613(1980)8<250:SFAVOR>2.0.CO;2.

Finnsen, H. 1767. *Efterretning om tildragelserne ved bjerget Hekla udi Island i April og følgende maaneder 1766.* Horrebow, C. (ed.). Kongelig Universitets Bogtrykker Andreas Hartvig Godicbe, Kjøbenhavn 1–46 pp.

Fulcher, G. S. 1925. Analysis of recent measurements of the viscosity of glasses. *J. Am. Ceram. Soc.* 8, 339–355.

Geirsson, H., P. LaFemina, T. Árnadóttir, E. Sturkell, F. Sigmundsson, M. Travis, P. Schmidt, B. Lund, S. Hreinsdóttir and R. Bennett 2012. Volcano deformation at active plate boundaries: Deep magma accumulation at Hekla volcano and plate boundary deformation in south Iceland. *J. Geophys. Res. Solid Earth* 117, B11409, https://doi.org/10.1029/2012jb009400.

Giordano, D., J. K. Russell and D. B. Dingwell 2008. Viscosity of magmatic liquids: A model. *Earth Planet. Sci. Lett.* 271, 123–134, https://doi.org/10.1016/-j.epsl.2008.03.038.

Gregg, T. K. P. and J. H. Fink 2000. A laboratory investigation into the effects of slope on lava flow morphology. *J. Volc. Geoth. Res.* 96, 145–159, https://doi.org/-10.1016/S0377-0273(99)00148-1.

Grönvold, K., G. Larsen, P. Einarsson, S. Thorarinsson and K. Saemundsson 1983. The Hekla eruption 1980–1981. *Bull. Volcanol.* 46, 349–363, https://doi.org/-10.1007/BF02597770.

Gudnason, J., Th. Thordarson, B. F. Houghton and G. Larsen 2018. The 1845 Hekla eruption: Grain-size characteristics of a tephra layer. *J. Volc. Geoth. Res.* 350, 33–46, https://doi.org/10.1016/-j.jvolgeores.2017.11.025.

Gudnason, J., Th. Thordarson, B. F. Houghton and G. Larsen 2017. The opening subplinian phase of the Hekla 1991 eruption: properties of the tephra fall deposit. *Bull. Volcanol.* 79(34), https://doi.org/10.1007/-s00445-017-1118-8.

Hack, A. C. and A. B. Thompson 2011. Density and Viscosity of Hydrous Magmas and Related Fluids and their Role in Subduction Zone Processes. *J. Petrology* 52, 1333–1362, https://doi.org/10.1093/-petrology/egq048.

Harris, A. J. L., J. B. Murray, S. E. Aries, M. A. Davies, L. P. Flynn, M. J. Wooster, R. Wright and D. A. Rothery 2000. Effusion rate trends at Etna and Krafla and their implications for eruptive mechanisms. *J. Volc. Geoth. Res.* 102, 237–269, https://doi.org/-10.1016/S0377-0273(00)00190-6.

Harris, A. J. L. and S. K. Rowland 2015. Lava Flows and Rheology. *The Encyclopedia of Volcanoes*, 17, Sigurdsson, H., B. Houghton, S. McNutt, H. Rymer and J. Stix (eds.), 321–342, Elsevier Inc., https://doi.org/-10.1016/B978-0-12-385938-9.00017-1.

Harris, Andrew J. L., M. Favalli, F. Mazzarini and C. W. Hamilton 2009. Construction dynamics of a lava channel. *Bull. Volcanol.* 71, 459–474, https://doi.org/-10.1007/s00445-008-0238-6.

Hon, K., J. Kauahikaua, R. Denlinger and K. Mackay 1994. Emplacement and inflation of pahoehoe sheet flows: Observations and measurements of active lava flows on Kilauea Volcano, Hawaii. *Geol. Soc. Am. Bull.* 106, 351–370, https://doi.org/10.1130/0016-7606(1994)106<0351:eaiops>2.3.co;2.

Houghton, B. F., D. A. Swanson, J. Rausch, R. J. Carey, S. A. Fagents and T. R. Orr 2013. Pushing the Volcanic Explosivity Index to its limit and beyond: Constraints from exceptionally weak explosive eruptions at Kilauea in 2008. *Geology* 41, 627–630, https://doi.org/-10.1130/G34146.1.

Hulme, G. 1974. The interpretation of lava flow morphology. *Geophys. J. Int.* 39, 361–383, https://doi.org/-10.1111/j.1365-246X.1974.tb05460.x.

Höskuldsson, Á., N. Óskarsson, R. Pedersen, K. Grönvold, K. Vogfjörð and R. Ólafsdóttir 2007. The millennium eruption of Hekla in February 2000. *Bull. Volcanol.* 70, 169–182, https://doi.org/10.1007/s00445-007-0128-3.

Jakobsson, S. P. 1979. Petrology of recent basalts of the Eastern Volcanic Zone, Iceland. *Acta Naturalia Islandica* 26, 1–103. http://hdl.handle.net/10802/4995.

Janebo, M. H., B. F. Houghton, Th. Thordarson and G. Larsen 2016. Shallow conduit processes during the ad 1158 explosive eruption of Hekla volcano, Iceland. *Bull. Volcanol.* 78(74), https://doi.org/-10.1007/s00445-016-1070-z.

Janebo, M. H., B. F. Houghton, Th. Thordarson, C. Bonadonna and R. J. Carey 2018. Total grain-size distribution of four subplinian-Plinian tephras from Hekla volcano, Iceland: Implications for sedimentation dynamics and eruption source parameters. *J. Volc. Geoth. Res.* 357, 25–38, https://doi.org/-10.1016/j.jvolgeores.2018.04.001.

Janebo, M. H., Th. Thordarson, B. F. Houghton, C. Bonadonna, G. Larsen and R. J. Carey 2016. Dispersal of key subplinian–Plinian tephras from Hekla volcano, Iceland: implications for eruption source parameters. *Bull. Volcanol.* 78, 1–16, https://doi.org/-10.1007/s00445-016-1059-7.

Kilburn, C. R. J. 2004. Fracturing as a quantitative indicator of lava flow dynamics. *J. Volc. Geoth. Res.* 132, 209–224, https://doi.org/10.1016/S0377-0273(03)00346-9.

Kolzenburg, S., D. Di Genova, D. Giordano, K. U. Hess and D. B. Dingwell 2018. The effect of oxygen fugacity on the rheological evolution of crystallizing basaltic melts. *Earth Planet. Sci. Lett.* 487, 21–32, https://doi.org/10.1016/j.epsl.2018.01.023.

Kolzenburg, S., D. Giordano, T. Thordarson, A. Höskuldsson and D. B. Dingwell 2017. The rheological evolution of the 2014/2015 eruption at Holuhraun, central Iceland. *Bull. Volcanol.* 79, https://doi.org/-10.1007/s00445-017-1128-6.

Kubanek, J., M. Westerhaus and B. Heck 2017. TanDEM-X Time series analysis reveals lava flow volume and effusion rates of the 2012–2013 Tolbachik, Kamchatka fissure eruption. *J. Geophys.*

Res. Solid Earth 122, 7754–7774, https://doi.org/-10.1002/2017JB014309.

Larsen, G., G. Sverrisdóttir, H. Jóhannesson, A. Hjartarson and P. Einarsson 2013. Hekla. *Náttúruvá á Íslandi*, University Press, Reykjavík, 189–209.

Larsen, G., A. Dugmore and A. Newton 1999. Geochemistry of historical-age silicic tephras in Iceland. *The Holocene* 9, 463–471, https://doi.org/-10.1191/095968399669624108.

Lucic, G., A. S. Berg and J. Stix 2016. Water-rich and volatile-undersaturated magmas at Hekla volcano, Iceland. *Geochem. Geophys. Geosyst.* 17, 3111–3130, https://doi.org/10.1002/2016gc006336.

Macdonald, G. A. 1953. Pahoehoe, aa and block lava. *Am. J. Sci.* 251, 169–191, https://doi.org/10.2475/-ajs.251.3.169.

Montalvo, J. 2013. *Evaluation of lava flow volumes from Hekla volcano based on new topographic data.* Master's thesis, Faculty of Earth Sciences, Univ. Iceland, 47 pp., http://hdl.handle.net/1946/17125.

Naranjo, M. F., S K. Ebmeier, S. Vallejo, P. Ramón, P. Mothes, J. Biggs and F. Herrera 2016. Mapping and measuring lava volumes from 2002 to 2009 at El Reventador Volcano, Ecuador, from field measurements and satellite remote sensing. *J. Appl. Volc.* 5(8), https://doi.org/10.1186/s13617-016-0048-z.

Ofeigsson, B. G., A. Hooper, F. Sigmundsson, E. Sturkell and R. Grapenthin 2011. Deep magma storage at Hekla volcano, Iceland, revealed by InSAR time series analysis. *J. Geophys. Res.* 116, https://doi.org/-10.1029/2010jb007576.

Parfitt, E. A. and L. Wilson 2008. *Fundamentals of Physical Volcanology.* Blackwell Publishing Ltd.

Pedersen, G. B. M., Á. Höskuldsson, T. Dürig, Th. Thordarson, I. Jónsdóttir, M. S. Riishuus, B. V. Óskarsson, *et al.* 2017. Lava field evolution and emplacement dynamics of the 2014–2015 basaltic fissure eruption at Holuhraun, Iceland. *J. Volc. Geoth. Res.* 340, 155–169, https://doi.org/10.1016/j.jvolgeores.2017.02.027.

Pedersen, G. B. M., J. M. C. Belart, E. Magnússon, O. K. Vilmundardóttir, F. Kizel, F. S. Sigurmundsson, G. Gísladóttir and J. A. Benediktsson 2018. Hekla volcano, Iceland, in the 20th century: lava volumes, production rates and effusion rates. *Geophys. Res. Lett.* 45, 1805–1813, https://doi.org/-10.1002/2017GL076887.

Pedersen, G. B. M., J. Montalvo, P. Einarsson, O. K. Vilmundardóttir, F. S. Sigurmundsson, J. M.-C. Belart, Á. R. Hjartardóttir, *et al.* 2018. Historical lava flow fields at Hekla volcano, South Iceland. *Jökull* 68, 1–26, http://jokulljournal.is/2018-68.html.

Peterson, D. W. and R. I. Tilling 1980. Transition of basaltic lava from pahoehoe to aa, Kilauea volcano, Hawaii: Field observations and key factors. *J. Volc. Geoth. Res.* 7, 271–293, https://doi.org/10.1016/0377-0273(80)90033-5.

Peterson, D. W., R. T. Holcomb, R. I. Tilling and R. L. Christiansen 1994. Development of lava tubes in the light of observations at Mauna Ulu, Kilauea Volcano, Hawaii. *Bull. Volcanol.* 56, 343–360, https://doi.org/-10.1007/BF00326461.

Pinkerton, H. and L. Wilson 1994. Factors controlling the lengths of channel-fed lava flows. *Bull. Volcanol.* 56, 108–120, https://doi.org/10.1007/BF00304106.

Poland, M. 2014. Time-averaged discharge rate of subaerial lava at Kilauea Volcano, Hawaii, measured from TanDEM-X interferometry: Implications for magma supply and storage during 2011-2013. *J. Geophys. Res. Solid Earth* 119, 5464–5481, https://doi.org/-10.1002/2014JB011132.

Portnyagin, M., K. Hoernle, S. Storm, N. Mironov, C. van den Bogaard and R. Botcharnikov 2012. H_2O-rich melt inclusions in fayalitic olivine from Hekla volcano: Implications for phase relationships in silicic systems and driving forces of explosive volcanism on Iceland. *Earth Planet. Sci. Lett.* 357–358, 337–346, https://doi.org/10.1016/j.epsl.2012.09.047.

Rizzoli, P., M. Martone, C. Gonzalez, C. Wecklich, D. B. Tridon, B. Bräutigam, M. Bachmann, *et al.* 2017. Generation and performance assessment of the global TanDEM-X digital elevation model. *ISPRS J. Photogrammetry and Remote Sensing* 132, 119–139, https://doi.org/10.1016/j.isprsjprs.2017.08.008.

Rowland, S. K. and G. P. L. Walker 1988. Mafic-crystal distributions, viscosities and lava structures of some Hawaiian lava flows. *J. Volc. Geoth. Res.* 35, 55–66, https://doi.org/10.1016/0377-0273(88)90005-4.

Saemundsson, K. 1978. Fissure swarms and central volcanoes of the neovolcanic zones of Iceland. In: Bowes, D. R. and B. E. Leake (eds.), Crustal evolution in northwestern Britain and adjacent regions, *Geol. J. Spec. Iss.* 10, 415–432.

Schythe, J. C. 1847. *Hekla og dens sidste udbrud den 2den September 1845.* Bianco Lunos Bogtrykkeri, Kjöbenhavn. 12–95.

Shaw, H. R. 1972. Viscosities of magmatic silicate liquids; an empirical method of prediction. *Am. J. Sci.* 272, 870–893, https://doi.org/10.2475/ajs.272.9.870.

Sigmarsson, O., M. Condomines and S. Fourcade 1992. A detailed Th, Sr and O isotope study of Hekla: differentiation processes in an Icelandic Volcano. *Contrib. Mineral. Petrol.*112, 20–34, https://doi.org/-10.1007/BF00310953.

Soosalu, H., P. Einarsson and S. Jakobsdóttir 2003. Volcanic tremor related to the 1991 eruption of the Hekla volcano, Iceland. *Bull. Volcanol.* 65, 562–577, https://doi.org/10.1007/s00445-003-0285-y.

Soule, S. A., K. V. Cashman and J. P. Kauahikaua 2004. Examining flow emplacement through the surface morphology of three rapidly emplaced, solidified lava flows, Kilauea Volcano, Hawaii. *Bull. Volcanol.* 66, 1–14, https://doi.org/10.1007/s00445-003-0291-0.

Stevens, N. F., G. Wadge and J. B. Murray 1999. Lava flow volume and morphology from digitised contour maps: a case study at Mount Etna, Sicily. *Geomorphology* 28, 251–261, https://doi.org/10.1016/S0169-555X(98)00115-9.

Sturkell, E., K. Ágústsson, A. T. Linde, S. I. Sacks, P. Einarsson, F. Sigmundsson, H. Geirsson, R. Pedersen, P. C. LaFemina and H. Ólafsson 2013. New insights into volcanic activity from strain and other deformation data for the Hekla 2000 eruption. *J. Volc. Geoth. Res.* 256, 78–86, https://doi.org/10.1016/-j.jvolgeores.2013.02.001.

Sverrisdottir, G. 2007. Hybrid magma generation preceding Plinian silicic eruptions at Hekla, Iceland: evidence from mineralogy and chemistry of two zoned deposits. *Geol. Mag.* 144, 643–659, https://doi.org/-10.1017/S0016756807003470.

Takagi, D. and H. E. Huppert 2010. Initial advance of long lava flows in open channels. *J. Volc. Geoth. Res.* 195, 121–126. https://doi.org/10.1016/-j.jvolgeores.2010.06.011

Thorarinsson, S. and G. E. Sigvaldason 1972. The Hekla Eruption of 1970. *Bull. Volcanol.* 36, 269–288, https://doi.org/10.1007/bf02596870.

Thórarinsson, S. 1976. The eruption of Hekla 1947–1948 IV: Course of events. *Soc. Sci. Islandica*, Reykjavík, 1–44.

Thórarinsson, S. 1967. The eruption of Hekla 1947–48 I: The eruptions of Hekla in historical times. A tephrochronological study. *Soc. Sci. Islandica*, Reykjavík, 1–171.

Thordarson, T. and G. Larsen 2007. Volcanism in Iceland in historical time: Volcano types, eruption styles and eruptive history. *J. Geodynamics* 43, 118–152, https://doi.org/10.1016/j.jog.2006.09.005.

Thordarson, T. and S. Self 1998. The Roza Member, Columbia River Basalt Group: A gigantic pahoehoe lava flow field formed by endogenous processes? *J. Geophys. Res. Solid Earth* 103, 27411–27445, https://doi.org/10.1029/98JB01355.

Thordarson, Th. 2000. Physical volcanology of lava flows on Surtsey, Iceland: A preliminary report. *Surtsey Research*, 11, 109–126.

Thordarson, Th. and Á. Höskuldsson 2008. Postglacial volcanism in Iceland. *Jökull* 58, 197–228.

Thy, P., C. E. Lesher, T. F. D. Nielsen and C. K. Brooks 2006. Experimental constraints on the Skaergaard liquid line of descent. *Lithos* 92, 154–180, https://doi.org/10.1016/j.lithos.2006.03.031.

Tuller-Ross, B., P. S. Savage, H. Chen and K. Wang 2019. Potassium isotope fractionation during magmatic differentiation of basalt to rhyolite. *Chemical Geology* (Elsevier BV) 525, 37–45, https://doi.org/-10.1016/j.chemgeo.2019.07.017.

Vogel, D. H. 1921. Temperaturabhängigkeitsgesetz der Viskosität von Flüssigkeiten. *Phys. Z.* 645–646.

Wadge, G. 1978. Effusion rate and the shape of aa lava flow-fields on Mount Etna. *Geology* 6, 503–506, https://doi.org/10.1130/0091-7613(1978)-6<503:eratso>2.0.co;2.

Wadge, G., G. P. L. Walker and J. E. Guest 1975. The output of the Etna volcano. *Nature* 255, 385–387, https://doi.org/10.1038/255385a0.

Walker, G. P. L. 1973. Lengths of Lava Flows. *Phil. Trans. Royal Soc. A: Mathematical, Physical and Engineering Sciences* 274, 107–118, https://doi.org/-10.1098/rsta.1973.0030.

Walker, G.P.L. 1991. Structure and origin by injection of lava under surface crust, of tumuli, "lava rises", "lava-rise pits", and "lava-inflation clefts" in Hawaii. *Bull. Volcanol.* 53, 546–558, https://doi.org/-10.1007/BF00298155.